LAWRENCE
LIVERMORE
NATIONAL
LABORATORY

LLNL-JRNL-796728

The Impact of the Third O2 Addition Reaction Network on Ignition Delay Times of neo-Pentane

N. Hansen, G. Kukkadapu, B. Chen, S. Dong, H. J. Curran, C. A. Taatjes, A. Eskola, D. L. Osborn, L. Sheps, W. J. Pitz, A. W. Jasper, W. Chen, J. Yang, Z. Wang, K. Moshammer

November 11, 2019

Proceedings of the combustion Institute

Disclaimer

This document was prepared as an account of work sponsored by an agency of the United States government. Neither the United States government nor Lawrence Livermore National Security, LLC, nor any of their employees makes any warranty, expressed or implied, or assumes any legal liability or responsibility for the accuracy, completeness, or usefulness of any information, apparatus, product, or process disclosed, or represents that its use would not infringe privately owned rights. Reference herein to any specific commercial product, process, or service by trade name, trademark, manufacturer, or otherwise does not necessarily constitute or imply its endorsement, recommendation, or favoring by the United States government or Lawrence Livermore National Security, LLC. The views and opinions of authors expressed herein do not necessarily state or reflect those of the United States government or Lawrence Livermore National Security, LLC, and shall not be used for advertising or product endorsement purposes.

The Impact of the Third O_2 Addition Reaction Network on Ignition Delay Times of *neo*-Pentane

N. Hansen,[1] G. Kukkadapu,[2] B. Chen,[3] S. Dong,[4] H. J. Curran,[4] C. A. Taatjes,[1] A. J. Eskola,[5] D. L. Osborn,[1] L. Sheps,[1] W. J. Pitz,[2] K. Moshammer,[6] A. W. Jasper,[7] W. Chen,[8] J. Yang,[8] Z. Wang[8]*

[1]Combustion Research Facility, Sandia National Laboratories, Livermore, CA 94551, USA

[2]Lawrence Livermore National Laboratory, Livermore, CA 94551, USA

[3]Institute for Combustion Technology, RWTH Aachen University, 52056 Aachen, Germany

[4]Combustion Chemistry Centre, Ryan Institute, MaREI, National University of Ireland, Galway, Ireland

[5]Department of Chemistry, University of Helsinki, FI-00560 Helsinki, Finland

[6]Physikalisch-Technische Bundesanstalt, Bundesallee 100, 38116 Braunschweig, Germany

[7]Chemical Sciences and Engineering Division, Argonne National Laboratory, Lemont, Illinois 60439, USA

[8]National Synchrotron Radiation Laboratory, USTC, Hefei, Anhui 230029, PR China

to be submitted to:

38th International Symposium on Combustion
"Gas-Phase Reaction Colloquium"

Word Count:	
Abstract:	236
Introduction:	575
Chemical Kinetic Model	315
Experimental Procedures	463
Results and Discussion:	2052
Summary and Conclusions:	231
Acknowledgements:	247
2 Tables	243
29 References:	542
7 Figures:	1532
Total:	**6200**

Color figures in electronic version only.

* Corresponding author: email: nhansen@sandia.gov; tel.: +1 925 294 6272

LLNL-JRNL-796728

Supplementary material is available.

The Impact of the Third O_2 Addition Reaction Network on Ignition Delay Times of *neo*-Pentane

N. Hansen,[1] G. Kukkadapu,[2] B. Chen,[3] S. Dong,[4] H. J. Curran,[4] C. A. Taatjes,[1] Arkke J. Eskola,[5] D. L. Osborn,[1] L. Sheps,[1] W. J. Pitz,[2] K. Moshammer,[6] A. W. Jasper,[7] W. Chen,[8] J. Yang,[8] Z. Wang[8]*

[1]Combustion Research Facility, Sandia National Laboratories, Livermore, CA 94551, USA
[2]Lawrence Livermore National Laboratory, Livermore, CA 94551, USA
[3]Institute for Combustion Technology, RWTH Aachen University, 52062 Aachen, Germany
[4]Combustion Chemistry Centre, Ryan Institute, MaREI, National University of Ireland, Galway, Ireland
[5]Department of Chemistry, University of Helsinki, FI-00560 Helsinki, Finland
[6]Physikalisch-Technische Bundesanstalt, Bundesallee 100, 38116 Braunschweig, Germany
[7]Chemical Sciences and Engineering Division, Argonne National Laboratory, Lemont, Illinois 60439, USA
[8]National Synchrotron Radiation Laboratory, USTC, Hefei, Anhui 230029, PR China

Abstract

We studied the oxidation of *neo*-pentane by combining experiments, theoretical calculations, and mechanistic developments to elucidate the impact of the 3rd O_2 addition reaction network on ignition delay time predictions. The experiments are based on photoionization mass spectrometry in jet-stirred and time-resolved flow reactors allowing for sensitive detection of the keto-hydroperoxide (KHP) and keto-dihydroperoxide (KDHP) intermediates. With *neo*-pentane exhibiting a unique symmetric molecular structure, which consequently results only in single KHP and KDHP isomers, theoretical calculations of ionization and fragment appearance energies and of absolute photoionization cross sections enabled the unambiguous identification and quantification of the KHP intermediate. Its temperature and time-resolved profiles together with calculated and experimentally observed KHP-to-KDHP signal ratios were compared to simulation results based on a newly developed mechanism that describes the 3rd O_2 addition reaction

LLNL-JRNL-796728

network. A satisfactory agreement has been observed between the experimental data points and the simulation results, thus adding confidence to the model's overall performance. Finally, this mechanism was used to predict ignition delay times reported previously in shock tube and rapid compression machine experiments [Bugler *et al.*, *Combust. Flame* 163 (2016), 138-156]. While the model accurately reproduces the experimental data, simulations with and without the 3rd O_2 addition reaction network included reveal only a negligible effect on the predicted ignition delay times at 10 and 20 atm. According to model calculations, low temperatures and high pressures promote the importance of the 3rd O_2 addition reactions.

Keywords: ignition delay times; third O_2 addition; *neo*-pentane; jet-stirred reactor; kinetic modeling

Introduction

It is now accepted that the low-temperature oxidation of hydrocarbon and oxygenated molecules is governed by successive radical additions to O_2 and intramolecular H-atom migration reactions that result in complex mixtures of many oxygenated radical and closed-shell intermediates [1, 2]. Kinetic schemes that include two O_2 additions to a radical and the formation and decomposition of a keto-hydroperoxide (KHP) intermediate are the basis for today's chemically detailed models for low-temperature oxidation [2]. Highly oxygenated intermediates containing up to two hydroperoxy groups, have recently been observed by Wang *et al.* in jet-stirred reactor experiments followed by mass spectrometric analysis [3-5]. They proposed a generalized reaction scheme in which a 3rd addition to O_2 leads to keto-dihydroperoxides (KDHP). A remaining question is whether these newly observed KDHPs and the 3rd O_2 addition steps influence fuel ignition.

The effect of the inclusion of reactions associated with a 3rd addition to O_2 in chemically detailed models on the prediction of ignition delay times (IDTs) was investigated for *n*-hexane [6]. It was shown that the effect on the IDT is strongly temperature dependent, *i.e.* at high temperatures the model showed that inclusion of the 3rd addition to O_2 resulted in only a negligible effect on the IDT, while at low temperatures a significant promotion of the IDT was observed. In this earlier work, the authors added 70 species and 151 reactions to a well-established *n*-hexane oxidation model using rates that were based on analogous reactions of the 2nd addition to O_2 reaction sequence. However, this example clearly shows that the number of conceivable species and their unknown kinetics make it difficult for both experiment and modeling to comprehensively understand the significance of the 3rd addition to O_2.

To overcome this challenge, *neo*-pentane is used as a fuel in this work. *neo*-Pentane (2,2-dimethyl propane) has a symmetric molecular structure in which all hydrogen atoms are identical and primary. At low-temperature combustion conditions, this simple molecular structure results in a concise reaction product distribution, *i.e.* only one isomeric form of the KHP [3-hydroperoxy-2,2-dimethylpropanal, HDMP, $HOOCH_2C(CH_3)_2CHO$] and of the KDHP [3-hydroperoxy-2-(hydroperoxymethyl)-2-methylpropanal, HHMMP, $(HOOCH_2)_2C(CH_3)CHO$] intermediates can be formed, as shown in Fig. 1. This property introduces an extra layer of constraints for kinetic modeling and makes *neo*-pentane an ideal

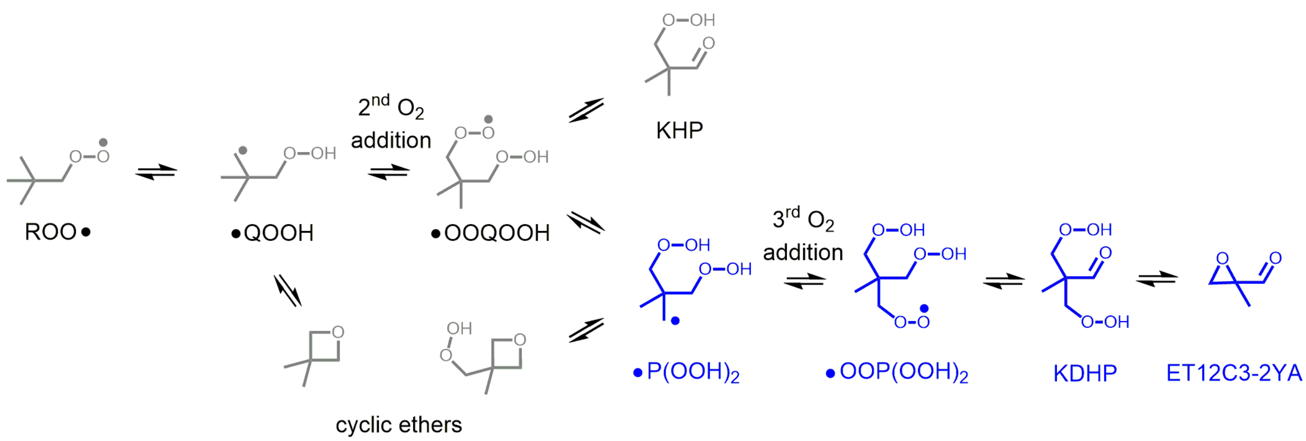

Figure 1: Low-temperature oxidation scheme of *neo*-pentane starting with the RO_2 radical and including 2nd and 3rd O_2 addition reactions, formation of cyclic ethers, KHP, and KDHP. As described below, chemical structures of the molecules that were newly added to the core mechanism are highlighted in blue. (56 mm×144 mm, 337 words)

candidate for elucidating the importance of the 3rd O_2 addition reaction network for IDTs.

The oxidation of *neo*-pentane has been studied before: For example, flow-reactor and jet-stirred reactor studies were carried out by Wang *et al.* [7], Eskola *et al.* [8], and Dagaut *et al.* [9]. The latest results concerning IDTs were provided by Bugler *et al.* [10, 11] who also presented a comprehensive chemical mechanism. Detailed mechanisms were also proposed in Refs. [12-14]. However, none of this earlier work was concerned with the 3rd O_2 addition reaction sequence. In this work, we used a coordinated combination of experiment, theory, and model development and calculations for elucidating the impact of the inclusion of the 3rd O_2 addition steps on the prediction of IDTs. The experiments, *i.e.* mass spectrometry after sampling from jet-stirred and flow reactors, together with theoretical calculations provide evidence for the KHP and KDHP. Their mole fraction profiles and signal intensities constrain a newly developed mechanism and allow for an assessment of its performance. This new mechanism is assembled based on a core mechanism from NUI Galway [10] that is extended to include 3rd O_2 addition sequences. Model predictions of IDTs at low temperatures reveal differences between the core and extended mechanism.

Chemical Kinetic Model

The chemical kinetic model for *neo*-pentane used for simulations in the current work is based on the detailed kinetic model of Bugler *et al.* [10], with the reaction rate of cyclic ether formation from QOOH slightly modified according to published alkane rate rules [15]. In detail, the rate for formation of cyclic ether has been perturbed within the known uncertainty of the calculations to improve the performance of the mechanism in predicting ignition delays. The perturbation was found not to affect the formation of KHP and KDHP nor did it affect the 3rd O_2 chemistry, which are the major focus of the current mechanism (c.f., Supplementary material). This kinetic mechanism, which we refer to as the “core mechanism”, describes the formation of the dihydroperoxy-alkyl radicals [$P(OOH)_2$] and the subsequent unimolecular decomposition reactions but does not include the 3rd O_2 addition reactions. As 3rd O_2 addition reactions are the focus of the current work, we added reactions to include the formation of the dihydroperoxy-alkylperoxy radicals [$O_2P(OOH)_2$] produced from 3rd O_2 additions. The $O_2P(OOH)_2$ radicals are modeled to produce KDHP along with OH radicals. The rates used for formation and consumption of $O_2P(OOH)_2$ radical and KDHP are taken from analogous rates in Bugler *et al.*’s mechanism. The newly added reactions are summarized in Table 1 and the newly assembled mechanism is referred to as “extended mechanism”. The newly added molecules are shown in Fig. 1 in blue. The stable intermediates produced from 3rd O_2 addition network are KDHP and ET12C3-2YA. KDHP consumption has been modeled by unimolecular decomposition reactions similarly to the consumption of KHP, and ET12C3-2YA consumption has been modeled using a simplified approach in which its oxidation is dominated by abstraction of weak aldehydic hydrogen. The base model (C_0−C_4) used in this study is NUIGMech1.0, which is developed at NUI Galway. It will be published soon and is available as Supplementary material.

Table 1: List of reactions and rate parameters added to the core mechanism

Reaction	A	n	E_a*	References and/or Comments
$NEOC_5H_9Q2+O_2=NEOC_5H_{11}O_6$	3.43E+16	-1.627	199	[16], A*0.5
$NEOC_5H_{11}O_6$=NEOC5KDHP+OH	10.36E+04	1.900	18800	[17], by analogy to $O_2CH_2CH_2CH_2OOH=HO_2CH_2CH_2CHO+OH$
NEOC5KDHP=OH+OH+CH_2O+ET12C3-2YA	3.00E+16	0.000	43000	[18]
ET12C3-2YA+O_2=CO+CH_3COCH_2+HO2	3.01E+13	0.000	39150	[19]
ET12C3-2YA+H=CO+$CH_3COCH_2+H_2$	1.31E+05	2.580	1220	[20]
ET12C3-2YA+O=CO+CH_3COCH_2+OH	5.94E+12	0.000	1868	H.J. Curran, fit to NIST database
ET12C3-2YA+OH=CO+$CH_3COCH_2+H_2O$	3.73E+04	2.600	-2300	Review of aldehyde+OH=RCO+H_2O
ET12C3-2YA+HO_2=CO+$CH_3COCH_2+H_2O_2$	3.01E+12	0.000	11920	[19]
ET12C3-2YA+CH_3=CO+$CH_3COCH_2+CH_4$	7.08E-04	4.580	1966	[21]

* kcal/mol

Experimental Procedures

The addition sequences to O_2 were studied experimentally using jet-stirred and laminar flow reactor facilities to obtain zero-dimensional and time-resolved information. The experiments were performed at the Advanced Light Source (ALS) of the Lawrence Berkeley National Laboratory and at the National Synchrotron Light Source (NSLS) of the University of Science and Technology of China in Hefei. In all three experiments, the intermediates are detected using mass spectrometry with single-photon ionization via synchrotron-generated vacuum-ultraviolet (VUV) radiation. This soft-ionization technique has been essential for the detection, identification, and quantification of highly-oxygenated species such as KHPs and KDHPs [1]. The individual set-ups have been described previously in detail [8, 22, 23] and only short descriptions are provided here.

The two JSR facilities at the ALS and at USTC are quite similar. They both consist of a quartz reactor that is typically operated at near-atmospheric pressure and that is coupled through a quartz sampling probe with a custom-built high-resolution reflectron time-of-flight mass spectrometer [22, 23]. The respective mass resolutions are sufficient to separate C/H/O containing molecules in the mass range of interest. The main differences between the two setups have been summarized in Ref. [1]. The mass spectrometers have a detection limit of ~ 1ppm. The three different flow conditions that were used for the JSR experiments are summarized in the Supplementary material.

A comprehensive mass spectrum is shown in the Supplementary material for the mass range from *m/z* = 65 to 135. The observed signal corresponds to intermediates and fragments following dissociative ionization processes. Given the intensities, the KDHP decomposition product, ET12C3-2YA, is most likely not significantly contributing to the observed $C_4H_6O_2$ signal.

Routines that employ theoretically calculated photoionization cross sections for converting the mass spectra into quantitative mole fractions have also been described previously [24, 25]. For comparison, an experimentally observed temperature trace of *neo*-pentane is shown in the Supplementary material together with the theoretically predicted profile.

The time-resolved kinetics experiments are carried out in a high-pressure laser photolytic reactor that uses pulsed-laser generation of Cl atoms to initiate oxidation of *neo*-pentane. This reactor also employs continuous sampling and synchrotron photoionization mass spectrometric analysis, as described in previous publications [8, 26]. The mass resolution of the spectrometer ($m/\Delta m$ ~ 1500) in the photolysis experiments is poorer than that of the reflectrons used in the JSR measurements. In these time-resolved laser-photolysis experiments, the analysis is confined to shorter residence times for which the second and third oxidation of product species can be minimized. As such, the JSR and flow reactor experiments are complementary, and the time response of certain signals can help identify dissociative ionization channels more easily, thus supporting the interpretation of the more complex JSR-sampled mass spectra. The time-resolved data on *neo*-pentane oxidation used throughout this paper have been reported earlier [8].

Results and Discussions

This section is organized as follows: First, we report the detection and identification of *neo*-pentane's KHP in the JSR experiments. Second, after quantification of the mass spectral KHP signal, this information is used, together with time-traces from the flow-reactor experiment, to assess the model's overall performance. Third, we report the detection of the keto-dihydroperoxide intermediate and use a semi-quantitative approach to verify that the extended mechanism's kinetic and thermodynamic data produce results that are consistent with the experimental observations. Finally, the chemically detailed core and extended mechanisms are used to predict IDTs from rapid compression machine and shock tube experiments at low- and high-temperature conditions that were reported earlier [10]. This analysis allowed for the elucidation of the importance of the 3rd O_2 addition sequences for IDTs.

Detection and Identification of the KHP

The parent ion of the HDMP, *neo*-pentane's KHP, is readily observable in the JSR-sampling mass spectrometric experiments at the exact mass-to-charge ratio of *m/z* = 118.063 ($C_5H_{10}O_3$). The $C_5H_{10}O_3$ photoionization efficiency (PIE) curve is shown in Fig. 2 and is in good agreement with the curve provided by Eskola *et al.* [8]. However, in the previous published work a detailed identification of the signal was not provided. It is shown in Fig. 2 that the experimentally observed ionization threshold of 9.05 (±0.1) eV (the gray box indicates the exp. uncertainty) is in good agreement with the calculated adiabatic ionization energy (8.95 eV; vertical arrow in Fig. 2). The gradual onset of the photoionization curve occurs over ~0.8 eV, which is similar to the range of the computed conformer-specific locally adiabatic ionization energies. The energies were calculated using levels of theory that have been used successfully in similar studies [24, 25]. In detail, M06-2X/cc-pVTZ geometries and frequencies and a high-level energy correction that approximates the CCSD(T)/CBS result, where ~CCSD(T)/CBS = CCSD(T)/cc-pVTZ + MP2/CBS – MP2/cc-pVTZ and the CBS limit was approximated using a two-point formula and the cc-pVTZ and cc-pVQZ basis sets. At this level of theory, the estimated uncertainty of the calculations is ±0.05 eV.

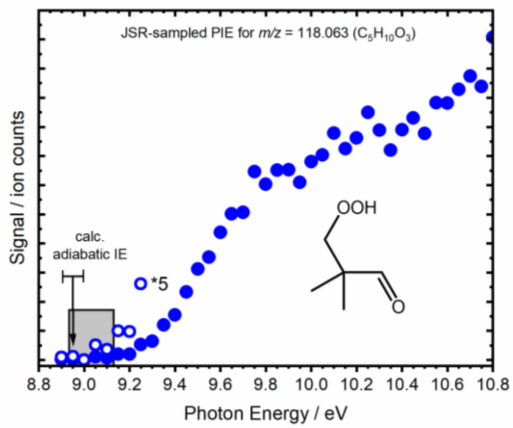

Figure 2: Photoionization efficiency curve of the intermediate at *m/z* = 118.063 ($C_5H_{10}O_3$). The observed ionization threshold matches the calculated adiabatic ionization energy. (56 mm×67 mm, 169 words)

Furthermore, the fragmentation pattern of HDMP was theoretically predicted based on channel energies as described by Moshammer *et al.* [25]. The results were compared with the experimentally observed appearance energies of the anticipated fragments (see Supplementary material). The results are summarized in Table 2.

Table 2: *neo*-Pentane's KHP [$HOOCH_2C(CH_3)_2CHO$] fragments: calculated and experimentally observed appearance energies.

Fragmentation Channel	Fragment *m/z*	Calculated AE, eV[a]	Experimentally observed AE, eV[a]
HOO-CH_2-$C(CH_3)_2H^+$ ($C_4H_{10}O_2^+$) + CO	90.068	9.41	9.40

HOO-CH_2-$C(CH_3)_2CO\cdot^+$ ($C_5H_9O_3^+$) + H	117.055	10.18	10.10
HOO-CH_2-$C(CH_3)_2\cdot^+$ ($C_4H_9O_2^+$) + ·CHO	89.060	10.44	10.50
·CH_2-$C(CH_3)_2CHO^+$ ($C_5H_9O^+$) + ·OOH	85.065	10.61	
·$C(CH_3)_2CHO^+$ ($C_4H_7O^+$) + ·CH_2OOH	71.050	10.70	
·O-CH_2-$C(CH_3)_2CHO^+$ ($C_5H_9O_2^+$) + ·OH	101.060	11.31	
HOO-CH_2-C·(CH_3)CHO^+ ($C_4H_7O_3^+$)+ ·CH_3	103.040	11.74	

[a]Estimated uncertainties: ±0.05 eV (theory) and ±0.1 eV (experiment)

Moreover, several of the dissociative ionization channels are corroborated by comparison to the time-resolved laser photolysis experiments, in which identical time traces can be used to correlate parent with fragment ions. For example, the time response of signal at *m/z* = 89 matches that at the KHP parent mass at *m/z* = 118, confirming a common origin.

Besides the exact mass and ionization and fragment appearance energies, further support for the assignment of the signal at *m/z* = 118.063 ($C_5H_{10}O_3$) to *neo*-pentane's KHP intermediate can be found in the temperature profile (as discussed below) of the mass spectral signal, which appears only in a small temperature range near 600 K. In summary, all experimental observations are consistent with the detection of the KHP structure, *i.e.*, $C_5H_{10}O_3$ can largely be identified as 3-hydroperoxy-2,2-dimethylpropanal (HDMP).

Quantification of the HDMP and assessment of the model's overall performance

To address the question about the impact of the 3rd O_2 addition reaction network, it is essential that the mechanism captures the sequential O_2 addition processes correctly. To test the model's performance with respect to accurately capturing the O_2 addition sequence, we compare the experimentally determined mole fraction profile of the HDMP with modeling calculations. The HDMP, which is a product of the first two O_2 addition and isomerization reactions, is a good indicator for the model's description of these first reaction steps.

To this end, we have converted the mass spectral signal of the KHP in the JSR experiments into temperature dependent mole fraction profiles using procedures that are based on calculated photoionization cross sections. Using a computational strategy previously described in Refs. [24, 25, 27], total photoionization cross sections of 7.12, 7.68, 8.32 and 8.92 Mb were calculated for HDMP at 0.1, 0.5, 1.0 and 1.5 eV above its ionization threshold of 9.0 eV, respectively. These values were then used to calibrate the experimental photoionization efficiency curve between 9.8 and 10.5 eV where a plateau region is clearly present, as shown in Fig. 3(a). The total cross section is the sum of the parent ion and the CO-loss fragmentation product, which, because of the observed intensities is the only fragmentation channel that needs to be taken into account. Based on this combined experimental and theoretical approach, a peak mole fraction of 1.8×10^{-4} at about 600 K has been determined, which compares favorably with the model predictions as shown in Fig. 3(b) for condition #3. The shaded area indicates the experimental uncertainty that can be traced back to uncertainties in the photoionization cross section, unexpected dissociative fragmentation, und calibrated instrument parameters, such as flow controllers, photodiode, and mass calibration.

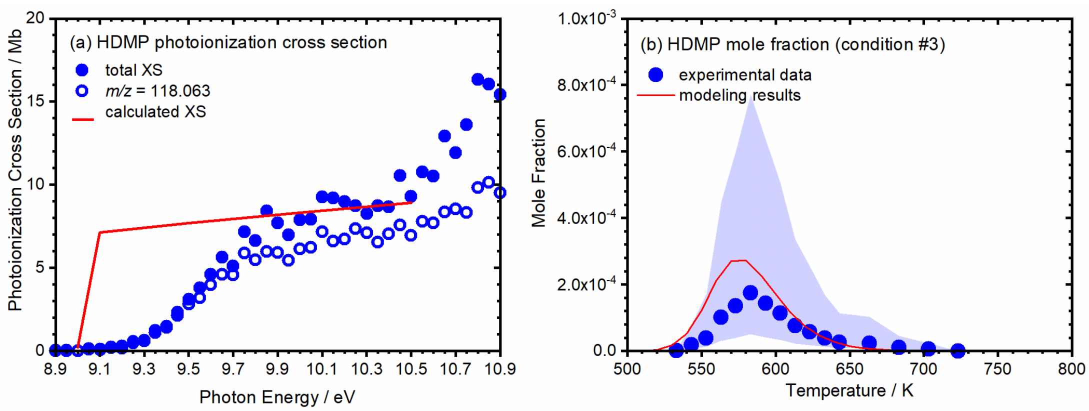

Figure 3: (a) Total ion signal (solid circles) of HDMP (parent ion and fragments) normalized to theoretically calculated photoionization cross sections (line). (b) Experimental mole fraction (solid circles) of HDMP as function of the temperature including experimental uncertainties for condition #3. The line represents the modeling results. (54 mm ×144 mm, 329 words)

The comparison of mole fraction profiles of other detected, identified, and quantified intermediates in the JSR experiments is outside the focus of the present paper and shall be discussed in a future publication. Instead, we test the extended mechanism against previously reported time-resolved data for the KHP intermediate from Ref. [8]. The favorable comparison of experimental and simulated results is shown in the Supplementary material for three different temperatures. Consistent with Ref. [8], we also included the same rate in the mechanism to account for wall loss reactions of the KHP. It should be noted that no quantitative information was provided in the previous work and that the modeling results have been scaled to match the signal intensity.

Detection of the keto-dihydroperoxide and identifying model constraints

The keto-dihydroperoxide ($C_5H_{10}O_5$) appears as a weak signal in the JSR-sampled mass spectra at *m/z* = 150.0528. A photoionization efficiency curve for this signal has not been recorded because a) the signal intensity would have been just too low to allow for an accurate interpretation of such a curve and b) the size of the molecules, *i.e.* it contains 10 heavy atoms, precludes the ready determination of the species ionization and fragment appearance energies. However, as outlined in the Introduction, there's only one possible $C_5H_{10}O_5$ KDHP isomer [3-hydroperoxy-2-(hydroperoxymethyl)-2-methylpropanal, HHMMP], and thus, for the remainder of this paper, we assume the detected signal at *m/z* = 150.0528 to be due to the HHMMP. The mass spectra of $C_5H_{10}O_3$ and $C_5H_{12}O_5$ are shown in Figs. 4(a) and (b), as detected after sampling from a 600K JSR at USTC (conditions #2). Similar mass spectra were observed at the ALS using slightly different conditions (conditions #1).

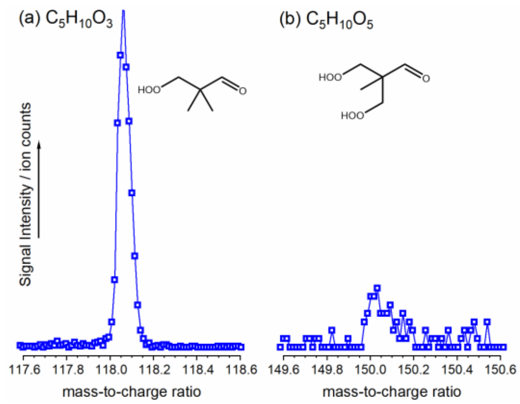

Figure 4: JSR-sampled mass spectra near *m/z* = 118 (a) and 150 (b) at 11.0 eV. While $C_5H_{10}O_3$ is identified as the keto-hydroperoxide (see text for details), it is assumed that the $C_5H_{10}O_5$ signal corresponds to the keto-dihydroperoxide. (52 mm×67 mm, 174 words)

While the mass spectral signal of the HHMMP is too weak to obtain a reliable mole fraction profile that can be compared to the model calculations, we follow a different approach here to constrain the chemically detailed mechanism. Single-temperature mass spectra were recorded for two different conditions at 590 and 600 K, respectively, for which HHMMP concentrations were predicted to be close to its maximum. And, after integration, the signal ratio of the parent ions of the KHP to the KDHP is used to verify the appropriateness of the kinetic and thermochemistry data in the extended mechanism. To this end, Fig. 5(a) shows the modeled KHP and KDHP signals for the two conditions studied in the two independent JSR experiments. As can be seen, for both conditions, the mole fractions peak around $1x10^{-3}$ and $2.5x10^{-5}$ for the HDMP and HHMMP intermediates and the ratio of the simulated mole fractions, which is strongly temperature-dependent, is shown in Fig. 5(b). The experimentally observed signal ratios of 36 and 42, respectively agree remarkably well the predictions of the model, thus adding confidence to the performance of the extended mechanism.

It should be kept in mind that this semi-quantitative approach is based on the assumptions that (a) most of the HDMP and HHMMP signal appears in the mass spectra at their respective parent ion masses and that (b) these two intermediates have similar photoionization cross sections. Based on our previous results and experiences, both assumptions seem reasonable: Fig. 3(a) indicates that the KHP intermediate is surprisingly stable upon photoionization compared to our previous work on the KHPs of dimethyl ether [22] and tetrahydrofuran [24, 26]. It is fair to assume that the HHMMP ion is also rather stable given that the HHMMP and HDMP have similar structural features. For the same reason, *i.e.* the same structural features, similar photoionization cross sections can be expected.

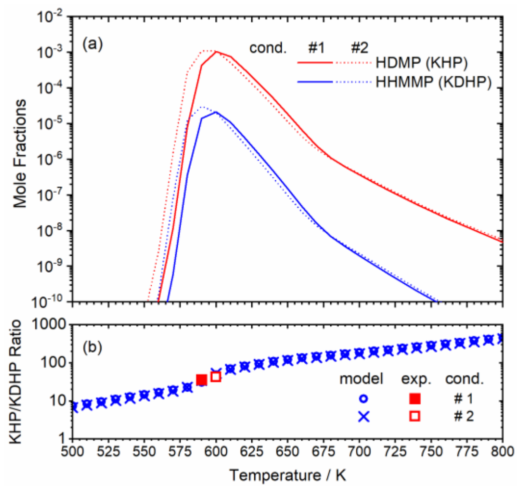

Figure 5: (a) Modeled mole fraction profiles of the keto-hydroperoxide and keto-dihydroperoxide as a function of temperature for both conditions. (b) Modeled KHP/KDHP mole fraction ratios compared to experimentally determined signal ratios. (63 mm×67 mm, 193 words)

To summarize: Based on the favorable comparison of the model's prediction with the quantitative analysis of the KHP, with the time-resolved KHP traces in the flow reactor experiments, and with the semi-quantitative analysis of the KDHP, it is fair to assume that the extended mechanism is capturing the reaction network of the O_2 addition sequences quite accurately.

Predicting ignition delay times and assessing the impact of the 3rd O₂ reaction sequences

This tested mechanism is then used to study the impact of the 3rd O_2 reaction network on the prediction of the IDTs. To this end, we have simulated the experiments that were described by Bugler *et al.* [10] using the core and the extended mechanism. Bugler *et al.* have used a shock tube (ST) and a rapid compression machine (RCM) to measure IDTs covering a range from 600-1800 K, pressures from 1, 10, and 20 atm, and stoichiometries from $\varphi = 0.5$ to 2.0. Because the 1 bar data were only reported for high temperatures, we consider here only pressures of 10 and 20 atm. Results for stoichiometries $\varphi = 1.0$ and 2.0 are shown in the Fig. 6, while $\varphi = 0.5$ results are included in the Supplementary material. The modeling results employing the mechanism with and without the 3rd O_2 reaction network are shown in Fig. 6 together with the previously reported experimental data. From Fig. 6, it is obvious that (a) the model is doing an extremely good job describing the experimental IDTs (thus providing more evidence for the mechanism's overall good performance) and that (b) inclusion of the 3rd O_2 reaction sequences does not change the prediction of the IDTs substantially at the chosen conditions. At high temperatures the predictions are identical, which can be traced back to the fact that KHP and KDHP appear only at the low temperature region. But even in that low-temperature region, only a minimal effect is observed. According to the current mechanism, 3rd O_2 addition reactions promote reactivity at high pressures and very low temperatures ($T < 650$ K), for e.g., a promotion of ignition delay times by nearly 30% is predicted at 600 K, 100 atm, and an equivalence ratio of 0.5 (see Supplementary material).

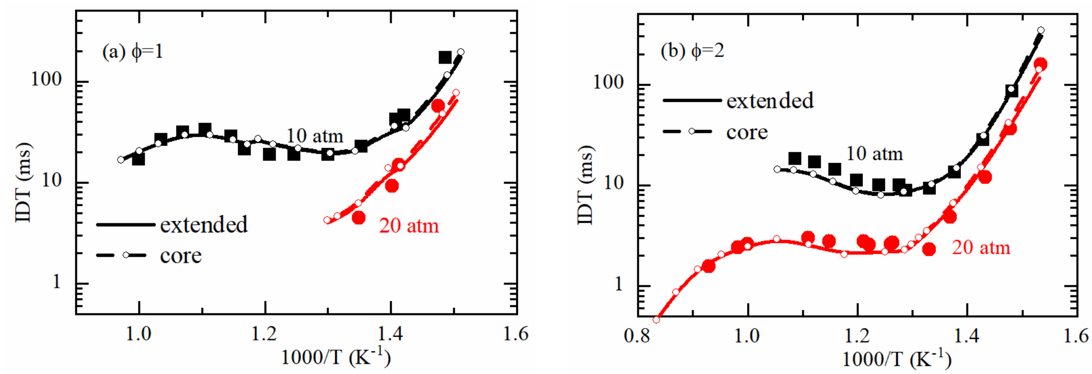

Figure 6: IDT simulations employing the chemically detailed mechanism with and without the 3rd O_2 reaction network are compared with experimental results from a shocktube and a rapid compression machine covering 10 and 20 atm and a temperature range from 600 to 1100 K, as reported in Ref. [10]. (52 mm×144 mm, 330 words)

These findings are in agreement with the conclusions on the effect of the 3rd O_2 reaction network from prior studies on *n*-pentane [6]. However, prior modeling work [6] using an *n*-hexane chemical kinetic mechanism [28] has shown a significant effect of the 3rd O_2 reaction network on IDTs at low temperatures, and the IDTs of *n*-hexane were observed to be lowered by a factor of two. To understand the source for this difference in the effect of the 3rd O_2 reaction network, we reanalyzed the effect of the 3rd O_2 reaction network on IDTs of *n*-hexane using the latest *n*-C_6 mechanism coupled with the 3rd O_2 reaction network from Ref. [6]. Interestingly, the effect of 3rd O_2 reactions on reactivity of *n*-hexane was found to be less severe, and moderate changes (~10-25%) in IDTs were observed. From this analysis, we conclude that the effect of 3rd O_2 reaction network on ignition propensity is small. Kinetic analysis was conducted to understand the reasons for the observed differences between the current work and the earlier work of Ref. [6]. We found the difference in observations to be due to the choice of rates used in Ref. [28] for formation of hydroperoxy-cyclic oxiranes (HPCO) from β–P(OOH)$_2$ which compete with 3rd O_2 additions at low temperatures. Specifically, the rate used in the mechanism of Ref. [28] for formation of HPCO at low temperatures (500-700 K) was 4-8 times lower than theoretical calculations from Miyoshi [16] and

Villano *et al.* [29]. Adopting the rates for formation of HPCO from Refs. [16, 29] without any modifications results in lowering of flux through 3rd O_2 additions, and thereby reducing their effect (see Supplementary material for more information).

Summary and Conclusions

Since the first observation of extensive auto-oxidation schemes in low-temperature oxidation processes, the importance of the newly observed 3rd O_2 addition channels was in question. Here, we showed that this reaction sequence appears to not be substantially important for accurately predicting IDTs of *neo*-pentane at pressure up to 20 atm. This conclusion is based on a coordinated experimental and modeling effort in which *neo*-pentane has been used as the hydrocarbon reactant. *neo*-Pentane is an interesting fuel to explore the 3rd O_2 addition reactions because of its symmetric structure, where only one KHP and one KDHP isomer exist. This limitation on the conceivable structures of the reactive intermediates allows for an accurate interpretation of the experimental data and for only a limited number of reactions in the chemically detailed mechanism. Compared to the previous study [6], in which 70 species were used in the *n*-hexane mechanism to describe the 3rd O_2 addition pathways, only four species were needed here to describe 3rd O_2 addition sequences in *neo*-pentane oxidation. To add confidence into the model's predictions, it was verified that the newly assembled extended mechanism describes the O_2 sequences accurately via comparison of modeled and experimental data concerning the formation of key intermediates such as KHP and KDHP.

This study focuses on a small, branched alkane and additional efforts are needed to extend the conclusions to larger, real fuel components.

Acknowledgements

This material is based upon work supported by the U.S. Department of Energy (DOE), Office of Science, Office of Basic Energy Sciences. Sandia National Laboratories is a multimission laboratory managed and operated by National Technology and Engineering Solutions of Sandia, LLC., a wholly owned subsidiary of Honeywell International, Inc., for the U.S. Department of Energy's National Nuclear Security Administration under contract DE-NA0003525. The Advanced Light Source is supported by the Director, Office of Science, Office of Basic Energy Sciences, of the U.S. DOE under Contract No. DEAC02-05CH11231. The work at Argonne is supported by the U.S. Department of Energy, Office of Science, Office of Basic Energy Sciences, Division of Chemical Sciences, Geosciences, and Biosciences under Contract No. DE-AC02-06CH11357 through the GPCP program. The work at LLNL was performed under the auspices of the U.S. Department of Energy (DOE), Contract DE-AC52-07NA27344 and was supported by the U.S. Department of Energy, Office of Basic Energy Sciences and Vehicle Technologies Office, program managers Wade Sisk, Kevin Stork, Mike Weismiller and Gurpreet Singh was conducted as part of the Co-Optimization of Fuels & Engines (Co-Optima) project sponsored by the DOE Office of Energy Efficiency and Renewable Energy (EERE), Bioenergy Technologies and Vehicle Technologies Offices. A.J.E. acknowledges support from the Academy of Finland, Grant No. 288377. The authors at NUI Galway would like to acknowledge Science Foundation Ireland for funding via project numbers 15/IA/3177 and 16/SP/3829. Work at USTC was supported by the National Natural Science Foundation of China (Grant 51976208).

References

[1] Z. Wang; O. Herbinet; N. Hansen; F. Battin-Leclerc, *Exploring hydroperoxides in combustion: History, recent advances and perspectives.* Prog. Energy Combust. Sci. 73 (2019) 132-181.

[2] H.J. Curran, *Developing detailed chemical kinetic mechanisms for fuel combustion.* Proc. Combust. Inst. 37 (1) (2019) 57-81.

[3] Z. Wang; S.Y. Mohamed; L. Zhang; K. Moshammer; D.M. Popolan-Vaida; V.S.B. Shankar; A. Lucassen; L. Ruwe; N. Hansen; P. Dagaut; S.M. Sarathy, *New insights into the low-temperature oxidation of 2-methylhexane.* Proc. Combust. Inst. 36 (1) (2017) 373-382.

[4] Z. Wang; D.M. Popolan-Vaida; B. Chen; K. Moshammer; S.Y. Mohamed; H. Wang; S. Sioud; M.A. Raji; K. Kohse-Höinghaus; N. Hansen; P. Dagaut; S.R. Leone; S.M. Sarathy, *Unraveling the structure and chemical mechanisms of highly oxygenated intermediates in oxidation of organic compounds.* Proc. Nat. Acad. Sci. 114 (50) (2017) 13102-13107.

[5] Z. Wang; L. Zhang; K. Moshammer; D.M. Popolan-Vaida; V.S.B. Shankar; A. Lucassen; C. Hemken; C.A. Taatjes; S.R. Leone; K. Kohse-Höinghaus; N. Hansen; P. Dagaut; S.M. Sarathy, *Additional chain-branching pathways in the low-temperature oxidation of branched alkanes.* Combust. Flame 164 (2016) 386-396.

[6] Z. Wang; S.M. Sarathy, *Third O_2 addition reactions promote the low-temperature auto-ignition of n-alkanes.* Combust. Flame 165 (2016) 364-372.

[7] S. Wang; D.L. Miller; N.P. Cernansky; H.J. Curran; W.J. Pitz; C.K. Westbrook, *A flow reactor study of neopentane oxidation at 8 atmospheres: experiments and modeling.* Combust. Flame 118 (3) (1999) 415-430.

[8] A.J. Eskola; I.O. Antonov; L. Sheps; J.D. Savee; D.L. Osborn; C.A. Taatjes, *Time-resolved measurements of product formation in the low-temperature (550–675 K) oxidation of neopentane: a probe to investigate chain-branching mechanism.* Phys. Chem. Chem. Phys. 19 (21) (2017) 13731-13745.

[9] P. Dagaut; M. Cathonnet, *Oxidation of neopentane in a jet-stirred reactor from 1 to 10 atm: An experimental and detailed kinetic modeling study.* Combust. Flame 118 (1-2) (1999) 191-203.

[10] J. Bugler; B. Marks; O. Mathieu; R. Archuleta; A. Camou; C. Gregoire; K.A. Heufer; E.L. Petersen; H.J. Curran, *An ignition delay time and chemical kinetic modeling study of the pentane isomers.* Combust. Flame 163 (2016) 138-156.

[11] J. Bugler; K.P. Somers; E.J. Silke; H.J. Curran, *Revisiting the kinetics and thermodynamics of the low-temperature oxidation pathways of alkanes: a case study of the three pentane isomers.* J. Phys. Chem. A 119 (28) (2015) 7510-7527.

[12] H.J. Curran; W.J. Pitz; C.K. Westbrook; M.W.M. Hisham; R.W. Walker, *An intermediate temperature modeling study of the combustion of neopentane.* Proc. Combust. Inst. (1996) 641-649.

[13] M. Ribaucour; R. Minetti; L. Sochet; H. Curran; W. Pitz; C. Westbrook, *Ignition of isomers of pentane: an experimental and kinetic modeling study.* Proc. Combust. Inst. 28 (2) (2000) 1671-1678.

[14] S. Taconnet; Y. Simon; G. Scacchi; F. Baronnet, *Experimental study and modeling of the oxidation reactions of neopentane and isopentane.* Can. J. Chem.-Rev. Can. Chim. 77 (7) (1999) 1177-1190.

[15] K. Zhang; C. Banyon; U. Burke; G. Kukkadapu; S.W. Wagnon; M. Mehl; H.J. Curran; C.K. Westbrook; W.J. Pitz, *An experimental and kinetic modeling study of the oxidation of hexane isomers: Developing consistent reaction rate rules for alkanes.* Combust. Flame 206 (2019) 123-137.

[16] A. Miyoshi, *Molecular size dependent falloff rate constants for the recombination reactions of alkyl radicals with O_2 and implications for simplified kinetics of alkylperoxy radicals.* Înt. J. Chem. Kin. 44 (1) (2012) 59-74.

[17] S. Sharma; S. Raman; W.H. Green, *Intramolecular hydrogen migration in alkylperoxy and hydroperoxyalkylperoxy radicals: accurate treatment of hindered rotors.* J. Phys. Chem. A 114 (18) (2010) 5689-5701.

[18] K. Sahetchian; R. Rigny; J.T. De Maleissye; L. Batt; M.A. Khan; S. Mathews, *The pyrolysis of organic hydroperoxides (ROOH).* Proc. Combust. Inst. 24 (1) (1992) 637-643.

[19] D. Baulch; C. Cobos; R. Cox; C. Esser; P. Frank; T. Just; J. Kerr; M. Pilling; J. Troe; R. Walker, *Evaluated kinetic data for combustion modelling.* J. Phys. Chem. Ref. Data 21 (3) (1992) 411-734.

[20] L.B. Harding; Y. Georgievskii; S. Klippenstein, *Roaming radical kinetics in the decomposition of acetaldehyde.* J. Phys. Chem. A 114 (2) (2009) 765-777.

[21] K. Gupte; J. Kiefer; R. Tranter; S. Klippenstein; L. Harding, *Decomposition of acetaldehyde: Experiment and detailed theory.* Proc. Combust. Inst. 31 (1) (2007) 167-174.

[22] K. Moshammer; A.W. Jasper; D.M. Popolan-Vaida; A. Lucassen; P. Diévart; H. Selim; A.J. Eskola; C.A. Taatjes; S.R. Leone; S.M. Sarathy; Y. Ju; P. Dagaut; K. Kohse-Höinghaus; N. Hansen, *Detection and identification of the keto-hydroperoxide ($HOOCH_2OCHO$) and other intermediates during low-temperature oxidation of dimethyl ether.* J. Phys. Chem. A 119 (28) (2015) 7361-7374.

[23] F. Battin-Leclerc; O. Herbinet; P.A. Glaude; R. Fournet; Z. Zhou; L. Deng; H. Guo; M. Xie; F. Qi, *Experimental confirmation of the low-temperature oxidation scheme of alkanes.* Angew. Chem. Int. Ed. 49 (18) (2010) 3169-3172.

[24] N. Hansen; K. Moshammer; A.W. Jasper, *Isomer-selective detection of keto-hydroperoxides in the low-temperature oxidation of tetrahydrofuran.* J. Phys. Chem. A 123 (38) (2019) 8274-8284.

[25] K. Moshammer; A.W. Jasper; D.M. Popolan-Vaida; Z. Wang; V.S. Bhavani Shankar; L. Ruwe; C.A. Taatjes; P. Dagaut; N. Hansen, *Quantification of the keto-hydroperoxide ($HOOCH_2OCHO$) and other elusive intermediates during low-temperature oxidation of dimethyl ether.* J. Phys. Chem. A 120 (40) (2016) 7890-7901.

[26] I.O. Antonov; J. Zádor; B. Rotavera; E. Papajak; D.L. Osborn; C.A. Taatjes; L. Sheps, *Pressure-dependent competition among reaction pathways from first- and second-O additions in the low-temperature oxidation of tetrahydrofuran.* J. Phys. Chem. A 120 (33) (2016) 6582-6595.

[27] A.C. Rousso; N. Hansen; A.W. Jasper; Y. Ju, *Low-temperature oxidation of ethylene by ozone in a jet-stirred reactor.* J. Phys. Chem. A 122 (43) (2018) 8674-86.

[28] K. Zhang; C. Banyon; C. Togbé; P. Dagaut; J. Bugler; H.J. Curran; Flame, *An experimental and kinetic modeling study of n-hexane oxidation.* Combust. Flame 162 (11) (2015) 4194-4207.

[29] S.M. Villano; L.K. Huynh; H.-H. Carstensen; A.M. Dean, *High-pressure rate rules for alkyl+ O2 reactions. 2. The isomerization, cyclic ether formation, and β-scission reactions of hydroperoxy alkyl radicals.* J. Phys. Chem. A 116 (21) (2012) 5068-5089.